

# Emergence of asymmetry in evolution

P.L. Várkonyi<sup>a,\*</sup>, G. Meszéna<sup>b</sup>, G. Domokos<sup>c</sup>

<sup>a</sup>Department of Mechanics, Materials and Structures, Budapest University of Technology and Economics, H-1521 Budapest, Hungary

<sup>b</sup>Department of Biological Physics, Eötvös University of Sciences, H-1117 Budapest, Hungary

<sup>c</sup>Department of Theoretical and Applied Mechanics, Cornell University, Ithaca, NY 14853-1503, USA

Received 23 May 2005

Available online 23 February 2006

## Abstract

We investigate symmetry-breaking bifurcation patterns in evolution in the framework of adaptive dynamics (AD). We define *weak* and *strong* symmetry. The former applies for populations where only the simultaneous reflection of all individuals is an invariant transformation. The symmetry is strong in populations where reflection of some, but not all, individuals leaves the situation unchanged. We show that in case of weak symmetry evolutionary branching can lead to the emergence of two asymmetric variants, which are mirror images of each other, and the loss of the symmetric ancestor. We also show that in case of strong symmetry, evolutionary branching can occur into a symmetric and an asymmetric variant, both of which survive. The latter, asymmetric branching differs from the generic branching patterns of AD, which is always symmetric. We discuss biological examples for weak and strong symmetries and a specific model producing the new kind of branching.

© 2006 Elsevier Inc. All rights reserved.

**Keywords:** Adaptive dynamics; Bilateral symmetry; Evolutionary branching

## 1. Introduction

Symmetry and asymmetry are central concepts in understanding both phylogeny and ontogeny of animals (Moore, 2001). Except for sponges, all animal taxa can be characterized either by ‘bilateral’ or by ‘radial’ symmetry of their basic body plan. This distinction is based on having one or several planes of reflection symmetry passing through the oral-aboral axis of the animal. The actual body structure is often less symmetric than the basic body plan due to secondary loss of symmetry. In particular, the left–right symmetry of the bilateral animals is rarely perfect. Different kinds of asymmetries emerge in different time scales of evolution. On one hand, asymmetric locations of some organs, as the heart, or the liver, are as old as the *Vertebrates* themselves. On the other hand, functional asymmetry of the human brain is probably very recent. We are interested in understanding the bifurcation

structure of such evolutionary transitions from reflection symmetry to asymmetry.

Evolution is inherently related to optimization. The fitness function of the first can be regarded as the analogue of the potential function of the second. An optimal structural design is often asymmetric even if the problem is characterized by a symmetric potential function. Bifurcations describing such asymmetric optima have been studied elsewhere (Várkonyi and Domokos, 2006).

Nevertheless, evolution is more than just optimization. In most cases, a pre-defined global fitness function would predict a single winner of selection; optimization itself is unable to explain the origin of biological diversity. To account for the coexistence of parallel branches of the evolutionary tree, one should take into account ‘frequency dependence’, i.e. the fact that the fitness function depends on the relative sizes of competing populations. In case of frequency dependence, evolution itself modifies the fitness function all the way. Consequently, one cannot rely on a global optimality criterion for predicting the outcome of evolution. According to the theory of adaptive dynamics (AD) (Dieckmann and Law, 1996; Metz et al., 1996; Geritz et al., 1997, 1998; Meszéna et al., 2005) directional

\*Corresponding author.

E-mail addresses: [vpeter@mit.bme.hu](mailto:vpeter@mit.bme.hu) (P.L. Várkonyi), [geza.meszena@elte.hu](mailto:geza.meszena@elte.hu) (G. Meszéna), [gd34@cornell.edu](mailto:gd34@cornell.edu) (G. Domokos).

evolution via small mutational steps still proceeds in the direction of the *current* fitness gradient. However, the ‘uphill’ evolution on the ‘fitness landscape’ is no longer guaranteed to end up at a local optimum, a local pessimum can be equally reached (Eshel, 1983; Taylor, 1989; Christiansen, 1991; Abrams et al., 1993). In the latter case, the theory predicts branching in the evolutionary process (Geritz et al., 1997, 1998).

Evolutionary branching can be initiated in two different ways (Metz et al., 1996; Geritz et al., 2004):

- I. In a constant environment evolution converges to a branching point and branches there immediately.
- II. The population evolves to an evolutionary stable strategy and waits there until an environmental change bifurcates this strategy to a branching point. Evolutionary branching occurs as a response to the modified conditions.

It is a general perception (c.f. punctuated equilibrium, Eldredge and Gould, 1972) that the bulk of evolutionary change is restricted to short transitional periods, i.e. most of the time evolution stops, and is waiting for an environmental change which will trigger the new phase of rapid evolution. This implies that the seemingly more complicated Scenario II. is more relevant for the real process (c.f. Geritz et al., 2004).

While the primary goal of AD theory is to demonstrate the possibility of evolutionary branching in a population, we will apply it with appropriate modifications for the problem of emergence of asymmetry. We have to take into account that ontogeny of a symmetric body plan is simpler (and more ancient) than that of an asymmetric one. Consequently, we assume *exact* body symmetry, as a starting point. Then, emergence of asymmetry can be initiated in two ways (analogous to the two categories of evolutionary branching above):

- I. A change in the developmental program allows body asymmetry (and asymmetry proves to be advantageous). This scenario can happen in *constant environment*.
- II. The possibility for asymmetry is already present and an *environmental change* makes asymmetry advantageous.

In principle, three possible scenarios for the evolutionary loss of symmetry can be considered (Fig. 1). In the simplest case, an initially symmetrical population evolves to be asymmetric. This scenario is not a branching and it can be fully described within the confines of the optimization picture of evolution.

In the second scenario, *two* asymmetric populations (which are symmetric mirror images of each other), emerge. If we assume a fixed potential (fitness function) then the slightest violation of the reflection symmetry between the two asymmetric populations would result in a temporary advantage of one of the populations and competitive loss

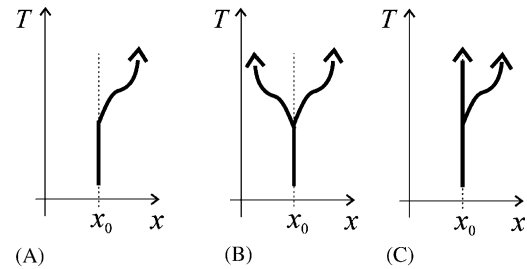


Fig. 1. Three fundamental patterns for the emergence of asymmetry (referred to as type (A), (B) and (C)).

of the other one. This scenario becomes robust only by assuming a frequency dependent fitness function.

The third scenario assumes a different kind of evolutionary branching. A new, asymmetric form speciates away from the original, symmetric one, however, the symmetric one survives as well. This scenario is inconceivable under the assumption of a fixed potential. On one hand, the asymmetric form cannot appear while the symmetric form is optimal, on the other hand, the symmetric form cannot survive when it becomes a local pessimum. Nevertheless, the scenario makes sense from the biological point of view: a new species acquires a new way of life and does not disturb its ancestor. Hence, frequency dependence is a necessary, however not sufficient ingredient of such situations. Any typical branching pattern is locally symmetric according to the conventional AD theory. Branching into a symmetric and an asymmetric branch is beyond the confines of the existing approach. As we will see, this type of evolution is made possible by the higher order terms, which are usually neglected, but become relevant here, as a consequence of the symmetry condition. The above three scenarios will be referred to henceforth as type (a), (b) and (c), respectively.

We summarize the necessary elements of AD for constant environment in Section 2. Section 3 introduces a distinction between two types of symmetry. Section 4 deals with possible scenarios for the emergence of asymmetry. Section 5 summarizes the patterns of evolutionary branching, Section 6 provides a model example. In the last section we review a few real-word cases.

## 2. Adaptive dynamics in constant environment

Here we summarize the essentials of AD theory in constant environment, following Geritz et al. (1997, 1998).

We consider evolution of a continuous inherited trait  $x$ , referred to as phenotype, or strategy. (Later we will identify this trait as the symmetry breaking parameter.) We assume that the investigated population is large and well-mixed, it may consist of several sub-populations with different strategies  $x_1, x_2, \dots, x_L$ . It is assumed that an underlying model specifies the joint dynamics of these strategies. We further assume that this dynamics reaches a unique, global and ‘simple’ attractor (i.e. fixed point, periodic or

quasi-periodic but not chaotic) on the fast time scale, except in degenerated cases (such as the coexistence of identical strategies).

From time to time, the dynamical system is perturbed by the emergence of a new, random ‘mutant’ strategy  $y$  with a small initial number of individuals. The mutant strategy  $y$  is always similar to an already existing one, which is considered as the ancestor of the mutant. The mutants appear on a slower time scale, i.e. when the already existing strategies have already reached the global fixed point.

The goal of AD is to understand the generic properties of the emerging evolutionary process, independently from the specific dynamical system governing the fast time scale changes of the populations.

### 2.1. Fitness concept

The fitness of a population is defined as its growth rate, i.e. the difference between the birth and the death rates. A population grows when its fitness is positive, i.e. when its rate of births is higher than its rate of deaths. In particular, one can assess the fitness of a newly emerged, and still rare, mutant strategy  $y$  when the ‘resident’ strategies  $x_1, x_2, \dots, x_L$  are in equilibrium. This fitness is the so-called ‘invasion fitness’  $s_{x_1, x_2, \dots, x_L}(y)$ . There are three possible scenarios with respect to the fate of strategy  $y$ :

- It spreads and the new equilibrium will contain this new strategy. (The transition may, or may not, involve extinction of some of the residents.) This case corresponds to positive invasion fitness, i.e.  $s_{x_1, x_2, \dots, x_L}(y) > 0$ .
- It becomes extinct ( $s_{x_1, x_2, \dots, x_L}(y) < 0$ ).
- Finding the consequences of the case  $s_{x_1, x_2, \dots, x_L}(y) = 0$  needs more detailed analysis. The mutant may spread, disappear or stay sparse according to higher order effects in density. This situation appears generically only in case of a linear fitness function (e.g. evolutionary game theory, c.f. Maynard-Smith, 1982, Meszéna et al., 2001.) or resource competition with substitutable resources (see e.g. Schreiber and Tobison, 2003). The latter case is not relevant for us.

Henceforth we will mainly concentrate on the invasion against a single resident, for which the invasion fitness  $s_x(y)$  trivially satisfies

$$s_x(x) = 0. \tag{1}$$

As a consequence of Eq. (1), the Taylor expansion of  $s_x(y)$  at  $(x, y) = (x_1, x_1)$ , in the variables  $\Delta x = (x - x_1)$  and  $\Delta y = (y - x_1)$ , can be written as

$$s_x(y)|_{x,y \approx x_1} = (\Delta y - \Delta x)(a_{00} + a_{10}\Delta x + a_{01}\Delta y + a_{20}\Delta x^2 + a_{11}\Delta x\Delta y + a_{02}\Delta y^2 + a_{30}\Delta x^3 + \dots). \tag{2}$$

The sign of the function  $s_x(y)$  can be conveniently plotted in a pairwise invasibility plot (PIP). (See Fig. 2(A) for an

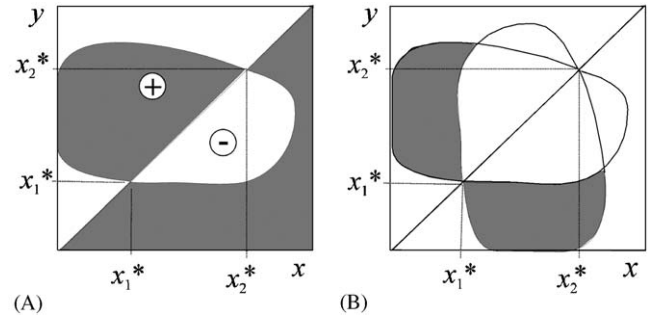


Fig. 2. (A) An example of the pairwise invasibility plot (PIP) with two singular strategies.  $x_1^*$  is neither convergence stable nor ESS,  $x_2^*$  is convergence stable and ESS. (B) The area of mutual invasibility.

example.) In this plot, horizontal and vertical axes correspond to the resident ( $x$ ) and the rare mutant ( $y$ ) strategies, respectively. The dark region represents the strategy combinations for which the mutant can spread against the resident, i.e.  $s_x(y) > 0$ . Observe that the main diagonal is always a borderline between the black and white regions, due to Eq. (1).

Fig. 2(B) represents mutual invasibility: gray region corresponds to strategy pairs  $(x, y)$  for which both  $s_x(y) > 0$  and  $s_y(x) > 0$ . The joint dynamics of such strategies should have an internal stable fixed point corresponding to positive number of individuals for both strategies, i.e. such a strategy pair  $(x, y)$  is able to coexist. Conversely (since we assumed that an internal attractor is globally attracting) coexistence implies the non-negativeness of the two growth rates. If the degenerated cases ( $s_x(y) = 0$  or  $s_y(x) = 0$ ) are not considered (c.f. the comments at the beginning of this subsection), coexistence implies mutual invasibility.

In many evolutionary models there exists a potential function  $W(y)$ , also referred to as fitness, with the property that the strategy with the larger potential outcompetes any strategy with a lower potential. This potential-optimization picture can be connected to the concept of invasion fitness via the identification

$$s_x(y) = W(y) - W(x), \tag{3}$$

i.e., the invasion fitness of a mutant corresponds to its advantage in potential-fitness. No mutual invasibility, i.e. no coexistence is possible in such models.

Evolutionary problems, which are characterized by an invasion fitness of type (3), are considered as frequency-independent, because fitness advantages/disadvantages do not depend on the relative frequencies (abundances) of the strategies. In this case,

$$\frac{\partial s_x(y)}{\partial x \partial y} = a_{10} - a_{01} = 0 \tag{4}$$

follows from (3).

2.2. Directional evolution

The direction of evolution via small mutational steps is determined by the ‘local fitness gradient’

$$D(x) = \left[ \frac{\partial s_x(y)}{\partial y} \right]_{y=x} = a_{00} \tag{5}$$

provided that it is non-zero. If  $D(x) > 0$ , a mutant with strategy  $y > x$  invades the resident population with strategy  $x$ , whereas if  $D(x) < 0$ , mutants with  $y < x$  can spread. Here we assume that  $|y - x|$  is small enough to guarantee that the linear term dominates the fitness advantage/disadvantage of the mutant. Moreover,  $s_x(y) \approx D(x)(y - x) > 0$  implies  $s_y(x) \approx D(y)(x - y) \approx D(x)(x - y) < 0$  in this context, i.e. the initial advantage of the mutant ensures that it ousts and replaces the resident, provided that  $D(x) \neq 0$ .

As newer and newer mutants arrive and replace their ancestors, this ‘trait substitution process’ constitutes a more-or-less continuous evolution in the direction determined by the local fitness gradient. See Dieckmann and Law (1996) for the deterministic approximation of this stochastic evolutionary process. This ‘directional’ evolution proceeds until a ‘singular’ strategy  $x^*$  is reached, for which  $D(x^*) = 0$ .

In a PIP, evolution to the positive direction is represented by having a black region immediately above the main diagonal (strategies between  $x_1^*$  and  $x_2^*$  in Fig. 2(A); see also Fig. 3B). Conversely, a black region immediately below the main diagonal represents evolution to the negative direction (strategies smaller than  $x_1^*$  or larger than  $x_2^*$  in Fig. 2; see also Fig. 3A). Consequently, singular strategies are characterized by intersection points of the main diagonal and another borderline (Fig. 3C–J).

2.3. Properties of singular strategies

Three distinct kinds of stability can be associated with singular strategies. A singular strategy  $x^*$  is a local attractor (or *convergence stable*) if and only if  $D(x)$ , which determines the direction of evolution, is positive for  $x < x^*$  and negative for  $x > x^*$  in the vicinity of the singular point. In the generic case, this yields the condition

$$\frac{dD(x)}{dx} \Big|_{x=x^*} = \frac{\partial^2 s_x(y)}{\partial y^2} \Big|_{y=x=x^*} + \frac{\partial^2 s_x(y)}{\partial x \partial y} \Big|_{y=x=x^*} = a_{10} + a_{01} < 0. \tag{6}$$

Note that a convergence stable singular strategy need not be a local fitness maximum. Strategy  $x^*$  is a local fitness maximum (or *evolutionary stable strategy*, (ESS)) in the generic case, if

$$\frac{\partial^2 s_x(y)}{\partial y^2} \Big|_{y=x=x^*} = a_{01} < 0. \tag{7}$$

Finally, a rare  $x^*$  strategist mutant can invade a population with slightly different strategy  $x$  ( $x^*$  is *invasion stable*), if  $s_x(x^*) > 0$ , which yields generically the condition

$$\frac{\partial^2 s_x(y)}{\partial x^2} \Big|_{y=x=x^*} = a_{10} < 0. \tag{8}$$

The three conditions coincide for frequency independent fitness by Eq. (4), but not in general. For example, there are singular strategies, which are convergence stable, but evolutionary unstable (Eshel, 1983; Taylor, 1989; Christiansen, 1991; Abrams et al., 1993)

At a *typical* singular strategy, the fitness function is dominated by the  $a_{10}$  and  $a_{01}$  coefficients, thus the local PIP contains two intersecting lines (one of these is the main diagonal), which divide the plot into four regions. (Later we will encounter cases when the first non-zero term is of higher order.) Fig. 3C–J represent the possible local configurations of the PIP around a singular strategy. The singular strategy is an ESS, if the vertical line through the intersection point lies in white regions (cases G–J) and it is invasion stable if it lies in the black part (cases C,D,I,J). Convergence stability is indicated by a black region above the main diagonal on the left side and below the main diagonal on the right (cases C,H–J).

The really important singular points are the convergence stable ones, because an evolving population does not come close to a convergence-unstable strategy. At the same time, if a population’s strategy is already  $x^*$ , the two other stability criteria determine its fate.

- If  $x^*$  is an ESS (cases G–J), it cannot be invaded by any similar mutant, i.e. it is a final rest point of the evolutionary process.
- If it is neither ESS nor invasion stable (cases E,F), similar mutants spread in a population of  $x^*$  strategists and the latter ones get extinct. (The overall result is generically divergence from  $x^*$  because the E and F type singularities are not convergence stable.)

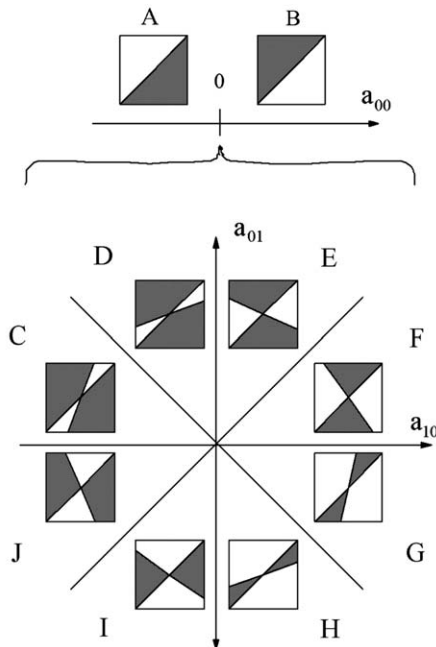


Fig. 3. Local PIPs around the point  $(x,x)$  at non-singular (A, B) and typical singular (C–J)  $x$  strategies.



- Finally, at an evolutionary unstable but invasion stable strategy (cases C,D), both the resident and the mutant are preserved and evolutionary branching occurs in such a way that both sub-populations diverge from the singularity. This branching process is discussed in Section 5. We remark that case D is usually not considered as a branching strategy, because its convergence instability prevents populations from converging to it, i.e. branching practically cannot occur.

### 3. Adaptive dynamics and symmetry

#### 3.1. Symmetry concept

Our goal is to describe symmetry-breaking via the evolution of an inherited continuous strategy  $x$ , in accordance with the framework of AD. Therefore we study evolution in the vicinity of a “symmetrical strategy”  $x_0$ , for which  $x_0 + \Delta x$  and  $x_0 - \Delta x$  strategists are reflections of each other for arbitrary  $\Delta x$ .

As illustration, consider a geometrical model of snail shell forms (Raup, 1962) with three parameters, one of which is the slope  $x$  of the spiral (Fig. 4). If  $x = 0$ , we have a curve in a plane, generating a flat shell, reflection-symmetric with respect to this plane. On the other hand, if  $x > 0$ , the shell is peaked and asymmetrical (dextral). With a negative value of  $x$ , the result is a reflected (sinistral) shell. In such a situation  $x = 0$  is a “symmetrical strategy”.

We already pointed out in Section 1 that the initial strategy of the evolving population is assumed to be exactly a symmetrical strategy. Beyond that, we assume in line with the AD methodology that the strategy  $x$  can be modified only by small mutation steps. In particular, we do not allow such “macro” mutations, via which ‘left-handed’ offspring of a ‘right-handed’ parent appear. See Section 6 for the consequences of some different assumptions.

#### 3.2. Two levels of symmetry

The question of evolutionary advantage/disadvantage of symmetry breaking is relevant only if the *environment* itself possesses the symmetry in question, that is, if replacing all individuals of the model by the reflected ones does not affect the model behavior. Two levels of symmetry can be distinguished in case of frequency dependence, i.e. when the interactions between the individuals affect the fitness function. We call a symmetrical strategy *strongly symme-*

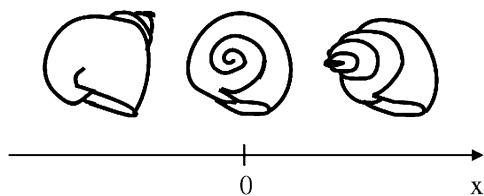


Fig. 4. An example of symmetrical strategies:  $x$  is the slope of the spiral axis of the shell.  $x > 0$  means dextral while  $x < 0$  means sinistral shell.

trical if all of the interactions are independent of left/right handedness. In this case, one can reflect some individuals, but not the others, and find the same model behavior. In contrast, if the interactions depend on the handedness of the affected individuals, only the simultaneous reflection of all individuals is an invariant transformation of the model. The latter situation will be referred to as *weak symmetry*.

On the level of invasion fitness, weak symmetry is represented by the relation

$$s_{x_0+\Delta x}(x_0 + \Delta y) = s_{x_0-\Delta x}(x_0 - \Delta y), \tag{9}$$

where  $\Delta x$  and  $\Delta y$  denote  $x - x_0$  and  $y - x_0$ , respectively. This symmetry condition implies that all terms of odd order vanish in the Taylor expansion of the invasion fitness function at  $x_0$ . That is, instead of Eq. (2), the expansion can be written as

$$s_x(y)|_{x,y \approx x_0} = (\Delta y - \Delta x)(a_{10}\Delta x + a_{01}\Delta y + a_{30}\Delta x^3 + a_{03}\Delta y^3 + a_{21}\Delta x^2\Delta y + a_{12}\Delta x\Delta y^2 + \dots). \tag{10}$$

Since  $a_{00}$  vanishes, the symmetrical strategy  $x_0$  is always singular. Since the coefficients  $a_{10}$  and  $a_{01}$  remain generically non-zero, the classification of the possible PIPs for a weak symmetry remains the same as in Fig. 3/C–J.

In contrast, the strong symmetry is characterized by a more restrictive condition:

$$s_{x_0+\Delta x}(x_0 + \Delta y) = s_{x_0+\Delta x}(x_0 - \Delta y) = s_{x_0-\Delta x}(x_0 + \Delta y). \tag{11}$$

In this case the general form of the invasion fitness function is

$$s_x(y)|_{x,y \approx x_0} = (\Delta y^2 - \Delta x^2)(b_{00} + b_{10}\Delta x^2 + b_{01}\Delta y^2 + b_{20}\Delta x^4 + b_{11}\Delta x^2\Delta y^2 + b_{02}\Delta y^4 + \dots). \tag{12}$$

The expansion contains only the terms, which are even in both variables, due to the more restrictive symmetry condition. Comparison with (10) yields  $a_{01} = a_{10} = b_{00}$  and similar relations for the higher order coefficients.

For strong symmetry,  $b_{00} < 0$  (Fig. 5/A) implies convergence, evolutionary and invasion stability, because

$$\frac{\partial^2 s_x(y)}{\partial x^2} \Big|_{y=x=x_0} + \frac{\partial^2 s_x(y)}{\partial x \partial y} \Big|_{y=x=x_0} = 2b_{00} + 0, \tag{13}$$

$$\frac{\partial^2 s_x(y)}{\partial y^2} \Big|_{y=x=x_0} = 2b_{00}, \tag{14}$$

$$\frac{\partial^2 s_x(y)}{\partial x^2} \Big|_{y=x=x_0} = -2b_{00}. \tag{15}$$

Such a strategy is an attractive endpoint of evolution. Conversely,  $b_{00} > 0$  leads to a singularity, which is unstable in all senses (Fig. 5B), i.e. it is a repellor.

Later, we will also be interested in the case of vanishing  $b_{00}$ . If  $b_{00} = 0$ , the character of the singular point is typically determined by  $b_{10}$  and  $b_{01}$  (Fig. 5/C–H). The six

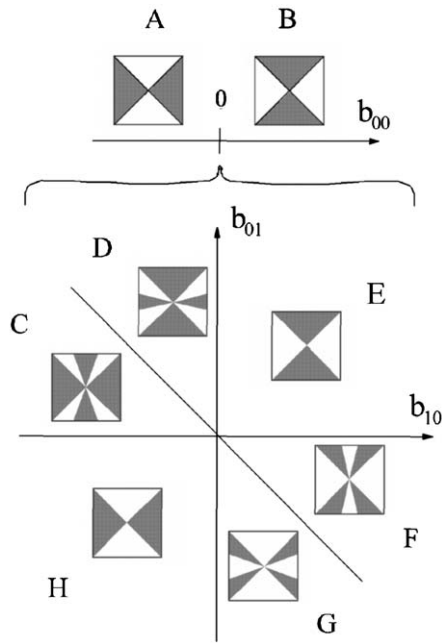


Fig. 5. Local PIPs for strong symmetry. A, B:  $x_0$  is a generic strongly symmetrical strategy ( $b_{00} \neq 0$ ); C–H:  $x_0$  is a degenerated strongly symmetrical strategy ( $b_{00} = 0$ ).

emerging configurations are partly invasion stable (C,D,H), partly ESS (F–H), and the two properties are not equivalent. In particular, C and D are *branching strategies*.

Note the geometrical interpretation of the two kinds of symmetry. Weak symmetry is equivalent to the fact that the PIP is invariant under a rotation of  $180^\circ$  around the point  $(x_0, x_0)$ . For strong symmetry, the PIP has a vertical and a horizontal symmetry axis at the point  $(x_0, x_0)$ . The weak and the strong symmetry are equivalent in frequency independent models, because frequency-independence means that the strategy of the competitors (including the handedness) does not affect the fitness of a strategy. Moreover, we have in this case

$$\frac{1}{4} \frac{\partial^4 s_x(y)}{\partial x^2 \partial y^2} = b_{10} - b_{01} = 0. \tag{16}$$

### 4. Emergence of asymmetry

In this section, we study the evolutionary loss of bilateral symmetry. We mentioned in Section 1 that it can occur in constant environment (case I) or it can be induced by environmental change (case II). In the latter case, we suppose that, initially, the symmetrical strategy is evolutionary stable and the population assumes this strategy. The phenomenon will be discussed separately for weak symmetry (Section 4.1), for strong symmetry without frequency dependence (Section 4.2) and for strong symmetry with frequency dependence (Section 4.3).

#### 4.1. Weak symmetry

We showed that the classification of generic weakly symmetrical strategies is the same as that of singular strategies without symmetry (Fig. 3). In constant environment (case I), asymmetry can emerge via type (a) divergence (c.f. Fig. 1) if the possibility of asymmetry develops when the population is at a repeller strategy (such as Fig. 3/E,F). Alternatively, type (b) branching may occur if asymmetry becomes reachable at a branching strategy (Fig. 3/C,D). Notice that evolution starts exactly from the singular point, so convergence stability is irrelevant and Fig. 3/D is also a branching point. The steps of this kind of branching process are summarized in Section 5 parallel with a different branching pattern.

Changing environment (case II) can be described by a moving point in the  $a_{10}$ - $a_{01}$  plane (Fig. 3), which is originally located in the ESS region. There are two generic possibilities for losing evolutionary stability: reaching the border in a non-invasion stable or in an invasion stable state (Fig. 6, cases 1 and 2). In case 1, type (a) divergence from the symmetrical strategy occurs, while in case 2, an ordinary (type (b)) evolutionary branching is initiated.

#### 4.2. Strong symmetry in frequency independent models

We have demonstrated in Section 2 that evolutionary and invasion stability are equivalent in frequency independent models and branching cannot occur. Thus asymmetry can only emerge via type (a) divergence from the symmetrical strategy in constant as well as in changing environment. (Divergence can be realized at Fig. 5/B type strategies.)

#### 4.3. Strong symmetry in frequency dependent models

Despite frequency-dependence, the ESS and the invasion stability conditions are *generically* equivalent at strongly symmetrical strategies. Thus, the common way of the emergence of asymmetry is of type (a), analogously to the

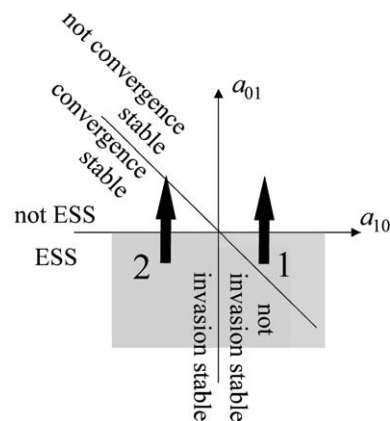


Fig. 6. The parameter plane for weak symmetry (the grey domain is ESS) and the two generic bifurcation events (1, 2).

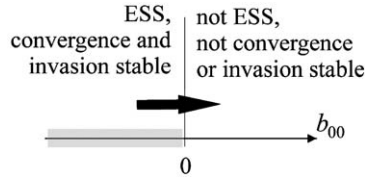


Fig. 7. The parameter line for strong symmetry. The grey domain is ESS, the arrow indicates bifurcation.

previous part. However, as the degenerate cases of Fig. 6/C–H break the equivalence, a different and surprising scenario may be realized in case II (changing environment) in presence of slow variation of  $b_{00}$ . The bifurcation process (Fig. 7) has the following main steps:

- Initially,  $b_{00} < 0$  and the symmetrical strategy is Fig. 5/A type (a stable evolutionary endpoint).
- The coefficient  $b_{00}$  approaches zero and one of the configurations of Fig. 5/C–H emerges temporarily.
- After some time,  $b_{00}$  gets far from zero on the positive side. The degenerate configuration disappears and the strategy becomes Fig. 5/B type (repellor).

If the mutation step would be infinitesimally small, the higher order terms would dominate the Taylor expansion (12) only for infinitesimally short period, not long enough to have any effect on the evolution of the population. However, we consider *small, but finite* steps in the strategy space. In this case the fourth-order terms dominate the quadratic ones in a finite interval of  $b_{00}$ , which may correspond to a long time interval, if the environmental change is sufficiently slow. Here evolutionary development of the population depends on the properties of the temporarily emerging, degenerate configuration:

- If the degenerate state is neither invasion stable nor an ESS (Fig. 5/E), type (a) divergence occurs as soon as the close-to-degenerate state is reached.
- If the degenerate state is an ESS (Fig. 5/F–H), the population stays symmetric, but later, as the degenerate state is replaced by a Fig. 5/B type repelling strategy, divergence occurs again.
- If the degenerate state is invasion stable but not evolutionary stable (Fig. 5/C,D) an evolutionary branching occurs in the close-to-degenerate state. In Section 5, we describe this branching process in detail and show that it is of type (c).

### 5. Novel way of evolutionary branching

The main goal of this section is to describe the details of the novel branching process of a population with *strongly symmetric* strategy, which was recognized in Section 4.3. (This is the situation  $b_{10} < b_{00} \approx 0 < b_{01}$ , see Fig. 5). This process differs significantly from the generic pattern of branching *without symmetry* (Geritz et al., 1998). We

describe the two ways of branching simultaneously to highlight the similarities and differences. Notice that the generic branching pattern in case of *weak symmetry* (Section 4.1) is the same as the latter one.

The steps of the two processes are collected in the left (standard case) and right (strongly symmetric case) column of Table 1. In both cases, row 1 presents the fitness functions before branching, row 2 shows why two evolving branches coexist, and row 3 presents the corresponding fitness functions. It is demonstrated in row 4, that the number of coexisting branches cannot be more than two. Finally the directions of evolution are determined in row 5.

In the standard case, the branching type evolution starts with the arrival of a mutant, which is located on the opposite side of the singularity  $x^*$  than the ancestor (row 2, left column). The consecutive mutation events always end up with extinction of the middle strategy (row 5, left column), i.e. two sub-populations evolve away from each other, resulting in a type (b) branching. In the strongly symmetric case, branching starts with the coexistence of a new, asymmetric mutant and its symmetric ancestors (row 2). The sequence of mutation-extinction steps results in a branching, in which one of the strategies stays symmetric while the other one evolves away; that is, a symmetric–asymmetric pair emerges in a type (c) branching (row 5, right column).

Evolution follows the introduced patterns as long as both sub-populations are close to the singular strategy. Later, the asymmetrical branch (at type (c) branching) or both branches (at type (b) branching) continue to evolve directionally according to their respective local fitness gradient, as demonstrated in Section 2.2 for a lone strategy.

### 6. A model example

In this section, we present a specific model to illustrate the type (c) branching. It is based on the examples of Levene (1953), Geritz et al. (1998). There are two parameters in the model,  $b$  and  $T$ , the latter representing the *time-dependence* of the model.

#### 6.1. Description of the model

Consider a population of  $x_1, x_2, \dots, x_n$  strategists, the number of the strategists is  $N_1, N_2, \dots, N_n$ , respectively. The model assumes non-overlapping generations, which live in a spatially heterogeneous environment consisting of *two different patches*. A limited number of individuals, denoted by  $K_1$  and  $K_2$ , live in each of the patches. The total number of individuals is constant:

$$N_1 + N_2 + \dots + N_n = K_1 + K_2. \quad (19)$$

The lifecycle of each generation consists of three parts.

- During dispersal, the offspring is distributed randomly in both patches; the frequency of a strategy  $x_k$  among

Table 1

The course of the branching process at a generic branching strategy  $x^*$  (standard case, left column), and the branching process emerging at a degenerated, strongly symmetric strategy  $x_0$  (right column)

	Standard case (Fig. 3/C)	Case of strong symmetry (Fig. 5/C,D)
1	The fitness function $s_{x^*}(y)$ , as a function of $y$ , has a minimum at $y = x^*$ . Locally, it can be approximated as (c.f. Eq. (2), Fig. 8/A). $s_{x^*}(y) \approx a_{01}(y - x^*)^2$ .	The fitness function $s_{x_0}(y)$ , as a function of $y$ , has a minimum at $y = x_0$ . Locally, it can be approximated as (c.f. Eq. (12), Fig. 9/A) $s_{x_0}(y) \approx b_{01}(y - x_0)^4$ .
2	Two strategies near to, but at the opposite sides of the singularity (i.e. $x_1 \leq x^* \leq x_2$ ) mutually invade each other and, consequently, are able to coexist.	If $x_1$ is near to $x_0$ , $x_1$ and $x_0$ mutually invade each other, i.e. they are able to coexist
3	If $x_1$ and $x_2$ are coexisting (c.f. row 2) and both of them are near to $x^*$ , the invasion fitness is $s_{x_1 x_2}(y) \approx a_{01}(y - x_1)(y - x_2)$ . (see Fig. 8(B), Eq. (2)), because $x_1, x_2 \approx x^*$ implies $s_{x_1 x_2}(y) \approx s_{x^*}(y)$ and $s_{x_1 x_2}(x_1) = s_{x_1 x_2}(x_2) = 0$ by definition.	If the $x_1 = x_0 + \Delta x_1$ and $x_0$ strategies are coexisting (c.f. row 2) and $x_1$ is near to $x_0$ , the invasion fitness has a double root at $x_0$ and two roots arranged symmetrically around $x_0$ : $s_{x_0 x_1}(y) \approx b_{01}(y - x_0)^2(y - x_0 - \Delta x_1)(y - x_0 + \Delta x_1)$ . (18) (see Fig. 9(B), Eq. (12)), because $x_1 \approx x_0$ implies $s_{x_0 x_1}(y) \approx s_{x_0}(y)$ , and $s_{x_0 x_1}(x_0) = s_{x_0 x_1}(x_1) = 0$ by definition, and finally $s_{x_0 x_1}(x_0 - \Delta x) = s_{x_0 x_1}(x_0 + \Delta x)$ for any $\Delta x$ , due to Eq. (11).
4	If more than two strategies coexisted, the corresponding fitness function would be 0 at each of them. The locally second-order invasion fitness function cannot have more than two zeroes, i.e. coexistence of more than two strategies is impossible in the vicinity of $x^*$ .	Generically only one strategy can coexist with $x_0$ , because the arrival of two strategies with exactly the same distance from $x_0$ ( $x_1 = x_0 + \Delta x, x_2 = x_0 - \Delta x$ ) is improbable and otherwise ( $x_1 = x_0 + \Delta x_1, x_2 = x_0 + \Delta x_2$ ) the fitness function should have zeros at $x_0 \pm \Delta x_1$ and $x_0 \pm \Delta x_2$ and a double root in $x_0$ . This is impossible, because it has only four roots in the vicinity of $x_0$ .
5	If a new mutant emerges in presence of a coexisting pair, one of the three should become extinct by row 4. The strategy becoming extinct should have a negative growth rate when it has become rare already. As $a_{01} > 0$ , this condition holds only for the middle strategy, i.e. if $x_1 < x_2 < x_3$ are the three strategies, $x_2$ will become extinct independently of which of them was the mutant. (Fig. 8(C))	When a new mutant appears at the equilibrium of $x_0$ and another strategy, one of the three strategies (i.e. $x_0, x_1 = x_0 + \Delta x_1$ and $x_2 = x_0 + \Delta x_2$ ) should become extinct by row 4. Assume that $ \Delta x_1  <  \Delta x_2 $ . Then $x_1$ will become extinct, because the strategy becoming extinct should have a negative growth rate when it has become rare already (Fig. 9(C)).

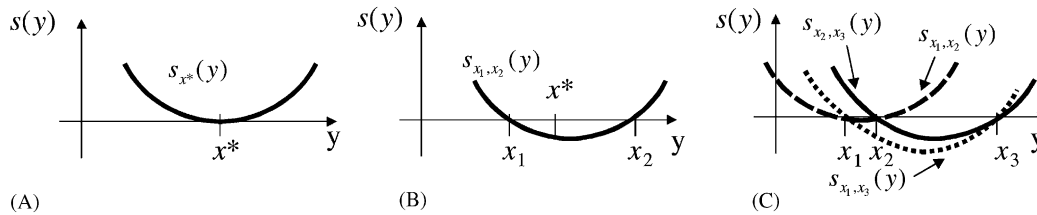


Fig. 8. Fitness of possible mutants at a standard branching strategy without symmetry. (A) before branching; (B) after branching; (C) fitness functions related to the coexistence of all pairs of strategies from  $x_1, x_2$  and  $x_3$ .

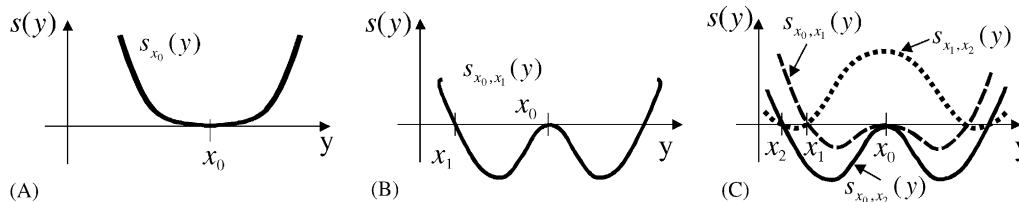


Fig. 9. Fitness of possible mutants at a degenerated, strongly symmetric branching strategy. (A) before branching; (B) if  $x_0$  and another strategy coexist; (C) fitness functions related to the coexistence of all pairs of strategies from  $x_0, x_1$  and  $x_2$ .

the offspring is proportional to the frequency of the parents with the same strategy, i.e. to  $N_k$ .

- In the second phase, the offspring is subjected to frequency-independent selection, which changes the

relative frequencies of the strategies in both patches independently. The chance of an  $x_k$  strategist in the  $i$ th patch of surviving this phase is proportional to a given function  $f_i(x_k)$ .



- In the third phase, the survivors spread in both patches until their numbers reach the capacities ( $K_1$  and  $K_2$ ) of the patches. The relative frequencies of the strategies in each of the patches are constant in this phase.

In this model, the chance of surviving the second phase is

$$f_1(x) = e^{-2b_1^2x^2 - x^4}, \quad (20)$$

$$f_2(x) = e^{2b_2^2x^2 - x^4} \quad (21)$$

with  $b_1$  and  $b_2$  positive parameters (see also Fig. 10). Since both functions are symmetrical,  $x = 0$  is a symmetrical strategy. Observe that this is an example of *strong symmetry*, hence there is no difference between  $x$  and  $-x$  strategists.

The optimal strategy is  $\pm b_2$  in the second patch, i.e. there is an *asymmetrical optimum*. In the first patch, there is a symmetrical optimum the ‘strength’ of which is determined by  $b_1$ .

Consider a rare mutant with strategy  $y$  in an equilibrium population of  $x_1, x_2, \dots, x_n$  strategists with equilibrium numbers  $\tilde{N}_1, \tilde{N}_2, \dots, \tilde{N}_n$ . If  $N_y$  is the (small) number of mutants in a generation, the  $N_{y'}$  number of mutants in the next generation can be approximated as

$$N_{y'} = K_1 \frac{f_1(y)N_y}{\sum_{k=1}^n f_1(x_k)\tilde{N}_k} + K_2 \frac{f_2(y)N_y}{\sum_{k=1}^n f_2(x_k)\tilde{N}_k}. \quad (22)$$

Consequently, the logarithmic per-capita growth rate of the rare mutants is

$$s_{x_1, x_2, \dots, x_n}(y) = \log\left(\frac{N_{y'}}{N_y}\right) = \log\left(K_1 \frac{f_1(y)}{\sum_{k=1}^n f_1(x_k)\tilde{N}_k} + K_2 \frac{f_2(y)}{\sum_{k=1}^n f_2(x_k)\tilde{N}_k}\right). \quad (23)$$

To reduce the number of model parameters, assume that  $b_1 = b_2 = b$  and let the parameter  $T$  be defined as

$$T = \frac{K_2}{K_1 + K_2}. \quad (24)$$

We can determine the fitness function of rare mutants in this model in case of a monomorphic resident population

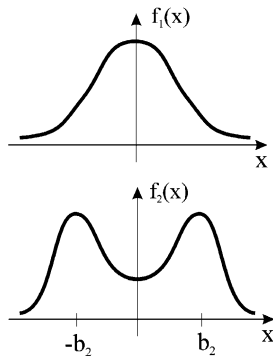


Fig. 10. The functions  $f_1(x)$  and  $f_2(x)$ .

(with strategy  $x$ ):

$$s_x(y) = \log\left[\left(1 - T\right)e^{-2b^2(y^2 - x^2) + x^4 - y^4} + T e^{2b^2(y^2 - x^2) + x^4 - y^4}\right]. \quad (25)$$

As it is expected, the fitness function satisfies the condition (11) of strong symmetry.

The results for the dimorphic case (two resident populations) are more involved. First, the equilibrium densities  $\tilde{N}_1, \tilde{N}_2$  of the two resident populations have to be determined from the following two equations:

$$\tilde{N}_i = K_1 \frac{f_1(x_i)\tilde{N}_i}{f_1(x_1)\tilde{N}_1 + f_1(x_2)\tilde{N}_2} + K_2 \frac{f_2(x_i)\tilde{N}_i}{f_2(x_1)\tilde{N}_1 + f_2(x_2)\tilde{N}_2} \quad \text{for } i = 1, 2. \quad (26)$$

Second, the results for  $\tilde{N}_1$  and  $\tilde{N}_2$  and Eqs. (20), (21) and (24) are substituted into (23) to obtain the fitness function. The results are quite complicated and they have to be analyzed numerically.

The fitness function for three or more coexisting strategies is uninteresting, since our analysis (in Section 6.2) shows that the maximal number of stably coexisting strategies is two.

### 6.2. Singular strategies and coalitions in the model

We investigated the behavior of the model at different values of  $b$  and  $T$ . Analysis of the fitness function (25) yielded the following results:

- $x_0 = 0$  is singular strategy, since it is a special symmetrical strategy.
- We determined the fitness gradient (see Eq. (5)) by deriving Eq. (25) with respect to  $y$ . Solving  $D(x^*) = 0$ , we found another pair of singular strategies:

$$x^*(b, T) = \pm b\sqrt{2T - 1} \quad \text{if } T > \frac{1}{2}. \quad (27)$$

- We analyzed the stability properties of the singular strategies by substituting Eq. (25) into the conditions (6) and (7). The  $x_0 = 0$  strategy is ESS, invasion and convergence stable if  $T < \frac{1}{2}$ , it is degenerate if  $T = \frac{1}{2}$  and it is unstable in all senses if  $T > \frac{1}{2}$ .
- The asymmetrical singular strategy is ESS invasion and convergence stable if  $b < 2^{-1/4}$ , or if  $b > 2^{-1/4}$  and  $T > T^*$  with

$$T^*(b) = \frac{1}{2} + \sqrt{\frac{1}{4} - \frac{1}{8b^4}}. \quad (28)$$

Otherwise it is a branching strategy (convergence and invasion stable but not ESS).

- In the degenerate state ( $T = \frac{1}{2}$ ) state, the stability of the symmetrical strategy can be determined from fourth derivatives of (25) with respect to  $x$  and  $y$ , which determine the  $b_{10}$  and  $b_{01}$  coefficients (see Eq. (12) and Fig. 5). The symmetrical strategy is ESS (Fig. 5/H type) if  $b < 2^{-1/4}$  and it is branching strategy (of type Fig. 5/C) if  $b > 2^{-1/4}$ .

Further, numerical computations showed that:

- There exists a convergence stable and ESS coalition of symmetrical  $x_1 = 0$  and asymmetrical  $x_2(b)$  strategists at appropriate parameter values.
- The value of  $x_2(b)$  is independent of  $T$ .
- The coalition exists if  $T_{min}(b) < T < T_{max}(b)$ . If  $T < T_{min}(b)$ , the asymmetrical strategy vanishes, while if  $T > T_{max}(b)$ , the symmetrical strategy gets extinct.

The PIP associated to the fitness function (25) is illustrated in Fig. 11 for some values of  $b$  and  $T$ . We can also construct an evolutionary bifurcation diagram of the model, which shows the singular strategies and coalitions at specific values of  $b$  (Fig. 12). We also plotted  $x_2(1)$ ,  $T_{min}(1)$  and  $T_{max}(1)$  in Fig. 12. For other values of  $b$ , the functions  $x_2(b)$  and  $T_{min}(b)$  can be determined numerically and  $T_{max}(b)$  is the solution of  $x_2(b) = x^*(b, T_{max}(b))$  (c.f. Eq. (27)).

### 6.3. Branching in the model

As we already showed, the model has a degenerate, symmetrical branching strategy at  $T = \frac{1}{2}$  and  $b > 2^{-1/4}$ . This means that a type (c) branching occurs at appropriate values of  $b$  (e.g.  $b = 1$ ), if the parameter  $T$  (representing the capacity of the second patch relative to the first one) slowly increases on evolutionary time scale and it reaches 1/2. Fig. 13(A), illustrates this branching in numerical simulations.

If the increase of  $T$  is faster, the model behavior is different: type (c) branching is replaced by type (a) divergence from the symmetrical strategy, followed by an ‘ordinary’ branching (Fig. 13(B)).

If  $b < 2^{-1/4}$ , no branching occurs. If  $T$  is increased and it reaches 1/2, the population diverges from the symmetrical strategy (type (a)) and converges to the asymmetrical singular strategy (Fig. 13(C)), which itself slowly moves with the increase of  $T$ .

At our example the increased speed of environmental change modified the pattern of the emergence of asymmetry (the type (c) branching of Fig. 13(A) was replaced by type (a) divergence and a standard branching in an asymmetrical state, as seen in Fig. 13(B)), but not the final outcome. There are other models where the higher speed of environmental change prevents branching, and modifies the evolutionary outcome as well.

### 7. Biological examples of symmetrical strategies

Some illustrative examples of strongly and weakly symmetrical strategies based on real-world populations are summarized in this section.

A widely known example of the secondary loss of bilateral symmetry is the beak of crossbills, which we introduce based on Benkman (1996), see also other works of the same author. The asymmetry of the beak is measured by the angle  $x$  of the lower mandible of crossbills:  $x = 0$ ,  $x < 0$  and  $x > 0$  correspond to straight,

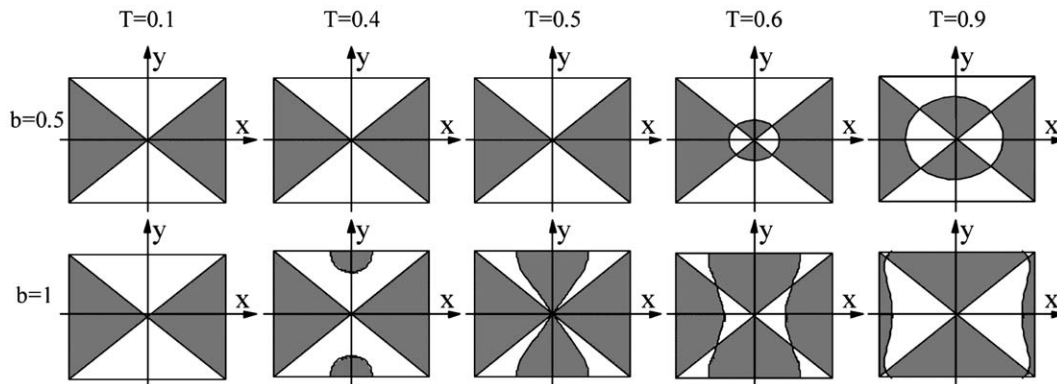


Fig. 11. PIP of the model at specific parameter values (the black region means positive fitness and the white means negative).

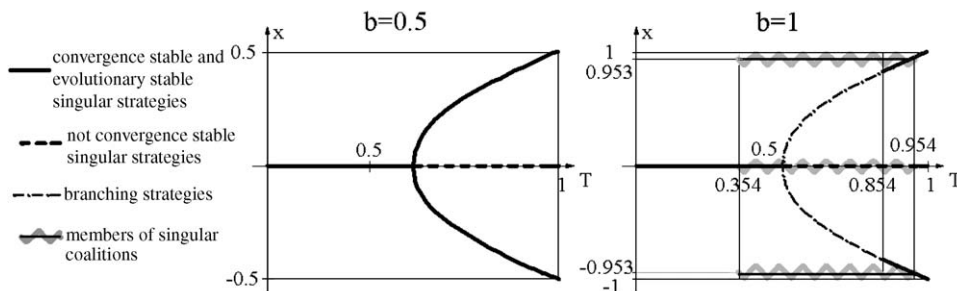


Fig. 12. Bifurcation diagram of the model at  $b = 0.5$  and  $b = 1$ .

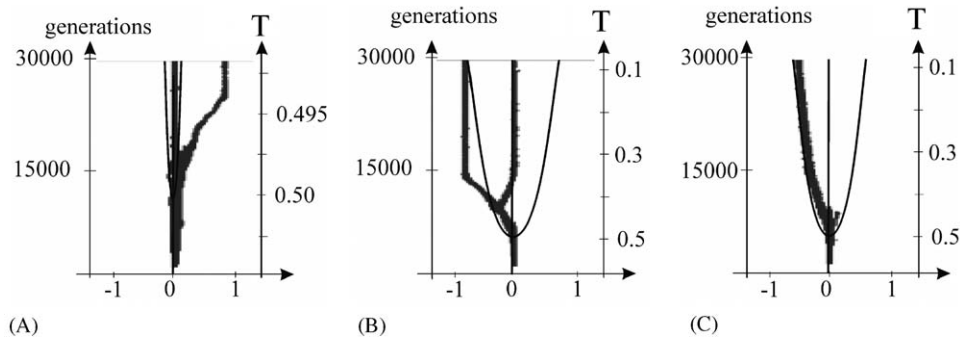


Fig. 13. Numerical simulations of the model. Thin lines indicate the monomorphic singular strategies in the model as functions of  $T$ . (A–B) With  $b = 1$  and different speeds of environmental changes ( $T$ ). In both cases, the two coexisting branches converge to the stable coalition  $(x_1; x_2) \approx (0; \pm 0.953)$ , c.f. Fig. 12/B. (C) With  $b = 0.5$ . Branching does not occur, evolution converges to the stable singular strategy.

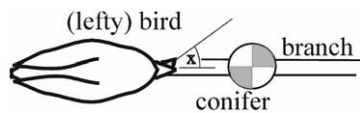


Fig. 14. Schematic upper view of a crossbill eating seeds from pine trees. The bird stands on the tree branch (on the left or right side of the conifer), and it can pick out the seeds from the two grey quarters of the conifer. (A righty crossbill could eat the seeds from the white quarters.)

leftward curved and rightward curved lower mandibles, respectively. Needless to say,  $x = 0$  is a symmetrical strategy.

Crossbills use their special beaks to pick out seeds from pinecones. Many of them, such as the White winged crossbill subspecies *Loxia leucoptera megaplaca* forage on pinecones, which cannot be twisted or removed from the trees (Fig. 14). Individuals can pick out seeds from only a part of the conifers depending on the direction of their beak. Thus, ‘lefties’ and ‘righties’ are ecologically *different*: the rarer one has ecological advantage in comparison with the more common one. The difference between lefties and righties is also indicated by the stable 1:1 ratio of the two morphs. This is an example of a *weak symmetry*. In contrast, the subspecies *Loxia leucoptera leucoptera* and *bifasciata* forage on different conifers, which are easily removed or twisted. In this case no ecological difference seems to exist between the two types of beaks. Accordingly, significant variance in the ratio of the two morphs was observed in different populations. This is an example for strong symmetry.

Different species of *Cichlid* fishes in Lake Tanganyika provide another pair of examples. The scale-eating *Perissodus microlepis* attack other species from behind and try to bite scales from the left or the right side of the victim (Takahashi and Hori, 1994). They have two asymmetrical forms in correspondence with the hunting strategy: Some of them open their mouth to the left, while the other ones have right-sided mouths. If  $x$  is the angle of mouth opening ( $x = 0$  for symmetrical mouth,  $x < 0$  for left-sided and  $x > 0$  for right-sided mouth),  $x = 0$  is again a *symmetrical* strategy. It is *weakly* symmetrical, because a

small group of  $-x$  in a big population of  $x$  strategists would have higher fitness than the frequent phenotype, because of the unexpected way of attacking the victims and the inequality  $s_x(-x) > 0$ , contradicting Eq. (11).

The herbivorous species *Telmatochromis temporalis* has similar, asymmetrical mouth, used to bite weed from the side of rocks while swimming along them (Mboko et al., 1998). As the weed does not adapt itself to the ‘hunting strategy’ of the fish, the  $x$  and  $-x$  strategists are ecologically equivalent in this case. Thus,  $x_0 = 0$  can be considered as a *strongly symmetrical* strategy.

More recent studies of Lake Tanganyika populations show, that the slightly asymmetrical body structure of many *Cichlid* species might have a different reason: it is an adaptive result of cross-predation in food chains. (Lefty predators tend to prefer righty victims and vice versa, see Nakajima et al., 2004). According to these results, all these species are examples of weak symmetry.

Finally, the shell chirality of snails, introduced in Section 3, becomes important at mating (Asami et al., 1998). The mating strategy of some *pulmonate* land snail species, which have relatively flat shells, prevents mating with individuals of opposite chirality, while a different mating behavior of other, tall-shelled species permits it. The different chirality has in the latter case only minor disadvantage according to experiments of Asami et al. (1998). The first situation is a typical example of weak symmetry and the second is close to strong symmetry (which would be perfect if there was no disadvantage of cross-mating at all).

## 8. Discussion

In this paper, we examined the evolutionary patterns of the emergence of secondary asymmetry in creatures with bilateral symmetry in their basic body plan. Three distinct scenarios have been described, as illustrated in Fig. 1. Two levels of bilateral symmetry (‘strong’ and ‘weak’) have been defined and the difference has been illustrated on biological examples. We determined the typical evolutionary patterns in different classes of models concerning symmetry.

Table 2

Types of emergence of asymmetry. Note that symmetry is always strong in absence of frequency dependence. (a), (b) and (c) refer to the scenarios of Fig. 1

	Weak	Strong
Non frequency-dependent		(a)
Frequency dependent	(a) (b)	(a) (c)

The results are summarized in Table 2: the type (a) emergence of asymmetry (when the superior asymmetrical form outcompetes the inferior symmetrical one) is possible in all three cases. Type (b) (when two asymmetrical variants emerge, avoiding competitive exclusion) requires weakly symmetrical frequency dependence. Finally, type (c) (when an asymmetrical form branches away from the unchanged and surviving symmetrical form) is restricted to the case of frequency-dependent strong symmetry.

Type (c) is a novel way of evolutionary branching. It differs from the usual pattern since the initial speed of divergence is not equal for the two branches. It relies on the transient dominance of the higher order terms, i.e. on a sufficiently slow change of the environmental parameters. We simulated this type of branching on a symmetrical version of Levene's classical multi-patch model.

Our study assumes that the size and direction of asymmetry (both determined by the phenotypic value  $x$ ) are inherited from the parents and mutations cause small deviation in  $x$ . In some cases, the direction of asymmetry develops randomly at some stage of the individual development (see Brown and Wolpert, 1990, Govind, 1989). This different inheritance mechanism would leave type (b) unchanged, and modify type (a) or (c) in such a way that a second asymmetrical branch with opposite handedness also appears.

It is also possible that, while handedness is inherited from parents, a special 'reflected' mutation (i.e. an offspring with opposite handedness) may occur with small probability. This is the case e.g. if the handedness is determined by a simple two-allele locus. If this type of mutation is frequent enough, again, the asymmetric variants will populate both asymmetric branches in types (a) and (c). However, if the reflected mutations are exceedingly rare, the relative frequencies of the lefties and the righties will change randomly.

This paper relies, and augments, the theory of AD. However, it has been pointed out in Section 1 that the emergence of asymmetry is initiated either by *change in the developmental program* or by *environmental change*. While neither plays a central role in the classical AD theory, one of these transitions is an essential element of the phenomenon investigated in this paper.

It is an ongoing debate in evolutionary biology whether AD itself is a proper description of the evolutionary process. (See, for instance, the target review by Waxman and Gavrilets (2005) and the related commentaries.) This

debate is about the relative importance of ecological and genetic factors in evolution (c.f. Schluter, 2001). According to the AD assertion, evolution must be considered in the context of ecologically induced frequency-dependence. We followed this tradition, which justifies considering any evolutionary phenomenon first in an asexual model. AD-based models with complete sexual genetics (e.g. Dieckmann and Doebeli, 1999) seem to support the possibility that speciation of sexual organisms is based on the phenomenon of AD-style evolutionary branching (Metz et al., 1996; Geritz et al., 2004). This concept is referred to as adaptive speciation (Dieckmann et al., 2004, see Gavrilets, 2005 for a criticism). While is beyond the confines of this paper to deal with this debate, we note the parsimony of this theory of "adaptive speciation": emergence of a new species is a direct adaptive consequence of the ecological possibility for this new species.

Adaptive speciation is often considered as an explanation for sympatric speciation, i.e. when no spatial segregation is involved (c.f. Via, 2001, Turelli et al., 2001). However, the idea is not restricted to the sympatric case, as several models, asexual as well as sexual ones, demonstrated evolutionary branching in spatial context (Meszena et al., 1997, Mizera and Meszena, 2003; Doebeli and Dieckmann, 2003). The model we presented in Section 5 belongs to this category also.

An interesting way to continue our research would be to detect the patterns of the emergence of asymmetry in Nature. The examples mentioned in Section 1 (asymmetry is of the human brain and the heart of vertebrates) seem to be frequency-independent, thus they emerged probably via scenario (a). Observations on the present state yield no evidence for the evolutionary pattern of the emergence of asymmetry in the past. Thus, with the exception of a few cases, empirical study of speciation is very difficult. While it is too slow for direct observation, simultaneously it is too fast to leave a fossil record (Eldredge and Gould, 1972). As a consequence, theoretical insight always played an important role in this field (Turelli et al., 2001). We contributed to this endeavor by investigating the bifurcation patterns of emergence of body asymmetry. We are intrigued to learn whether the novel way of evolutionary branching we uncovered is a part of the natural process of evolution.

## Acknowledgments

We thank . Kisdi, J. A. J. Metz, Tom Van Dooren and Claus Ruffler for discussions. The support of OTKA grants TS049885 and T049689 is gratefully acknowledged.

## References

- Abrams, P.A., Matsuda, H., Harada, Y., 1993. Evolutionarily unstable fitness maxima and stable fitness minima of continuous traits. *Evol. Ecol.* 7, 465–487.



- Asami, T., Cowie, R.H., Ohbayashi, K., 1998. Evolution of mirror images by sexually asymmetric mating behaviour in hermaphroditic snails. *Am. Nat.* 152, 225–236.
- Benkman, C.W., 1996. Are the ratios of bill crossing morphs in crossbills the result of frequency-dependent selection? *Evol. Ecol.* 10, 119–126.
- Brown, N.A., Wolpert, L., 1990. The development of handedness in left/right asymmetry. *Development* 109 (1), 1–9.
- Christiansen, F.B., 1991. On conditions for evolutionary stability for a continuously varying character. *Am. Nat.* 138, 37–50.
- Dieckmann, U., Doebeli, M., 1999. On the origin of species by sympatric speciation. *Nature* 400, 354–357.
- Dieckmann, U., Law, R., 1996. The dynamical theory of coevolution: a derivation from stochastic ecological processes. *J. Math. Biol.* 34, 579–612.
- Dieckmann, U., Doebeli, M., Metz, J.A.J., Tautz, D. (Eds.), 2004. *Adaptive Speciation*. Cambridge University Press, Cambridge.
- Doebeli, M., Dieckmann, U., 2003. Speciation along environmental gradient. *Nature* 421, 259–264.
- Eldredge, N., Gould, S.J., 1972. Punctuated equilibria: an alternative to phyletic gradualism. In: Schopf, T.J.M. (Ed.), *Models In Paleobiology*. Freeman, Cooper and Co., San Francisco.
- Eshel, I., 1983. Evolutionary and continuous stability. *J. Theor. Biol.* 103, 99–111.
- Gavrilets, S., 2005. Adaptive speciation: it is not that simple. *Evolution* 59, 696–699.
- Geritz, S.A.H., Kisdi, É., Meszéna, G., Metz, J.A.J., 1997. The dynamics of adaptation and evolutionary branching. *Phys. Rev. Lett.* 78, 2024–2027 ; Url: <http://angel.elte.hu/~geza/GeritzPRL.pdf>.
- Geritz, S.A.H., Kisdi, É., Meszéna, G., Metz, J.A.J., 1998. Evolutionary singular strategies and the evolutionary growth and branching of the evolutionary tree. *Evol. Ecol.* 12, 35–57.
- Geritz, S.A.H., Kisdi, É., Meszéna, G., Metz, J.A.J., 2004. Adaptive dynamics of speciation. In: Dieckmann, U., Doebeli, M., Metz, J.A.J., Tautz, D. (Eds.), *Adaptive Speciation*. Cambridge University Press, Cambridge.
- Govind, C.K., 1989. Asymmetry in lobster claws. *Am. Sci.* 77, 468–474.
- Levene, H., 1953. Genetic equilibrium when more than one niche is available. *Am. Nat.* 87, 331–333.
- Maynard-Smith, J., 1982. *Evolution and the Theory of Games*. Cambridge University Press, Cambridge.
- Mboko, S.K., Kohda, M., Hori, M., 1998. Asymmetry of mouth-opening of a small herbivorous Cichlid fish *Telmatochromis Temporalis* in lake Tanganyika. *Zool. Sci.* 15, 405–408.
- Meszéna, G., Czibula, I., Geritz, S.A.H., 1997. Adaptive dynamics in a 2-patch environment: a toy model for allopatric and parapatric speciation. *J. Biol. Syst.* 5, 265–284 ; Url: <http://angel.elte.hu/~geza/MeszenaEtal1997.pdf>.
- Meszéna, G., Kisdi, E., Dieckmann, U., Geritz, S.A.H., Metz, J.A.J., 2001. Evolutionary optimization models and matrix games in the unified perspective of adaptive dynamics. *Selection* 2, 193–210.
- Meszéna, G., Gyllenberg, M., Jacobs, F.J., Metz, J.A.J., 2005. Link between population dynamics and dynamics of Darwinian evolution. *Phys. Rev. Lett.* 95 (7), 078105 ; Url: [http://angel.elte.hu/~geza/PhysRevLett\\_95\\_078105.pdf](http://angel.elte.hu/~geza/PhysRevLett_95_078105.pdf).
- Metz, J.A.J., Geritz, S.A.H., Meszéna, G., Jacobs, F.J.A., van Heerwaarden, J.S., 1996. Adaptive dynamics, a geometrical study of the consequences of nearly faithful reproduction. I. In: van Strien, S.J., Verduyn Lunel, S.M. (Eds.), *Stochastic and Spatial Structures of Dynamical Systems*. Elsevier, North Holland, pp. 183–231.
- Mizera, F., Meszéna, G., 2003. Spatial niche packing, character displacement and adaptive speciation along an environmental gradient. *Evol. Ecol. Res.* 5, 1–20.
- Moore, J., 2001. *An Introduction to Invertebrates*. Cambridge University Press, Cambridge.
- Nakajima, M., Matsuda, H., Hori, M., 2004. Persistence and fluctuation of lateral dimorphism in fishes. *Am. Nat.* 163, 692–698.
- Raup, D.M., 1962. Computer as aid in describing form in gastropod shells. *Science* 138, 150–152.
- Schluter, D., 2001. Ecology and the origin of species. *Trends Ecol. Evol.* 16, 372–380.
- Schreiber, S.J., Tobianson, G.A., 2003. The evolution of resource use. *J. Math. Biol.* 47, 56–78.
- Takahashi, S., Hori, M., 1994. Unstable evolutionary stable strategy and oscillation: a model of lateral asymmetry in scale-eating cichlids. *Am. Nat.* 144, 1001–1020.
- Taylor, P.D., 1989. Evolutionary stability in one-parameter models under weak selection. *Theor. Popul. Biol.* 36, 125–143.
- Turelli, M., Barton, N.H., Coyne, J.A., 2001. Theory of speciation. *Trends Ecol. Evol.* 16, 330–343.
- Via, S., 2001. Sympatric speciation in animals: the ugly duckling grows up. *Trends Ecol. Evol.* 16, 381–390.
- Várkonyi, P.L., Domokos, G., 2006. Symmetry, optima and bifurcations in structural design. *Nonlinear Dynam.* 43, 47–58.
- Waxman, D., Gavrilets, S., 2005. 20 questions on adaptive dynamics: a target review. *J. Evolution. Biol.* 18, 1139–1154.